Thermochimica Acta 498 (2010) 112–116

Contents lists available at ScienceDirect

Thermochimica Acta

journal homepage: www.elsevier.com/locate/tca

Thermal, physicochemical and microstructural studies of organic analog of nonmetal–nonmetal monotectic alloy

K.P. Sharma, R.S.B. Reddi, Shiva Kant, R.N. Rai*

Department of Chemistry, Banaras Hindu University, Varanasi 221005, India

ARTICLE INFO

Article history:
Received 18 August 2009
Received in revised form 8 October 2009
Accepted 12 October 2009
Available online 20 October 2009

Keywords:
Phase diagram
Thermal properties
Monotectic alloys
Solid–liquid interfacial energy
Microstructure

ABSTRACT

The phase equilibrium of an organic analogue of a nonmetal–nonmetal system, involving resorcinol (R)–1,4-diiodobenzene (DIB), was established which shows solid is in equilibrium with liquid as well as two immiscible liquid phases are also in equilibrium with a liquid of single phase. The phase diagram study infers the formation of a monotectic and a eutectic at 0.05 and 0.97 mole fractions of resorcinol, respectively. Using X-ray diffraction technique, the range of solid solubility of R in DIB and DIB in R was studied. The thermal properties of materials such as heat of mixing, entropy of fusion, roughness parameter, interfacial energy and excess thermodynamic functions were computed from the enthalpy of fusion values, determined using differential scanning calorimeter (DSC) method. The solid–liquid interfacial energy shows the applicability of non-wetting condition. The effect of solid–liquid interfacial energy on morphological change of monotectic growth has also been discussed. The microstructures of monotectic, eutectic and pure components were taken and have shown their peculiar characteristic features.

1. Introduction

The mechanism of solidification behaviours of polyphase alloys, particularly monotectic alloys, are of potential importance for fundamental and industrial applications such as self-lubricating alloys [1,2]. In spite of an interesting area of investigations, metallic systems [3–5] are not suitable for detail study due to wide density difference, opacity and high transformation temperature of the components involved. However, low transformation temperature, transparency, wider choice of materials and minimised convection effects are the special features that have prompted a number of research groups [6–8] to work on organic eutectics, monotectics and molecular complexes. As such organic systems are used as model systems for detailed investigation of several parameters which control the mechanism of solidification and decide the properties of materials. From last two decades organic materials are considered for various physicochemical investigations to be used for non-linear optical and different other electronic applications [9–11].

The monotectic alloys have been less studied due to several difficulties associated with systems forming monotectic. Nonetheless, some of the articles [1,12,13] explain various interesting phenomena of monotectic alloys. The wide freezing range and large density difference between two liquid phases are the main problem. Thus, the role of wetting behaviour, interfacial energy, thermal conductivity and buoyancy during the phase separation process has been a subject of great discussion. Resorcinol and 1,4-diiodobenzene both are the materials of high enthalpy of fusion (22.20 and 24.13 kJ mol^{-1}, respectively) and simulates the nonmetallic solidification, therefore the present system is very good organic analog of nonmetal–nonmetal systems. In the present paper, the details concerning phase diagram, the range of solid solution formation, thermochemistry, linear velocity of crystallization at different undercoolings, heat of fusion, Jackson's roughness parameter, interfacial energy and microstructures are reported.

2. Experimental

2.1. Materials and purification

Resorcinol (Thomas Baker, India) was purified by crystallization from hot water while 1,4-diiodobenzene (Aldrich, Germany) was purified by crystallization from ethanol. The melting temperatures of R and DIB were found to be 110.5 and 130.0 °C, respectively which are consistent to their reported values [14,15].

2.2. Phase diagram

The phase diagram of R–DIB system was studied by determining the melting point temperature of mixtures of different composi-

* Corresponding author at: Department of Chemistry, Banaras Hindu University, Faculty of Science, Varanasi, UP 221005, India. Tel.: +91 542 6701597; fax: +91 542 2368127.
E-mail address: rn_rai@yahoo.co.in (R.N. Rai).

0040-6031/$ – see front matter © 2009 Elsevier B.V. All rights reserved.
doi:10.1016/j.tca.2009.10.010

tions of R–DIB and curve was plotted in composition and their respective melting temperature. In this method [16,17], mixtures of two components covering the entire range of compositions were prepared and these mixtures were homogenized by repeating the process of melting followed by chilling in ice cooled water 4–5 times. The melting/complete miscible temperature of different compositions were determined using a melting point apparatus attached with a precision thermometer associated with an accuracy of ±0.5 °C.

2.3. X-ray diffraction

To study the miscibility range of composition of DIB and R, that produces the solid solution, the X-ray diffraction (XRD) data were collected using Rigaku, D/max-2500/PC, Japan, X-ray diffraction unit. The samples of interest were scanned from 10° to 70° with a scanning rate of 4°/min [18].

2.4. Enthalpy of fusion

The heat of fusion of the pure components, the eutectic and the monotectic were determined [19] by differential scanning calorimeter (Mettelar DSC-4000 system). Indium sample was used to calibrate the DSC unit. The amount of test sample and heating rate were about 7 mg and 55 °C min^{-1}, respectively. The values of enthalpy of fusion are reproducible with in ±1.0%

2.5. Growth kinetics

The growth influence of temperature on growth kinetics of R, DIB and their eutectic and monotectic were studied [17,19] by measuring the rate of movement of the solid–liquid interface at different undercoolings in a capillary tube (U-shape) of 150 mm horizontal portion and 5 mm internal diameter. Molten samples of pure components, eutectic and monotectic were separately taken in a capillary and placed in a silicone oil bath. The temperature of oil bath was maintained using microprocessor temperature controller of accuracy ±0.15 °C. At a particular temperature, below the melting point of the sample, a seed crystal of the same composition was added to start nucleation and the rate of movement of the solid–liquid interface was measured using a traveling microscope and a stop watch.

2.6. Microstructure

Microstructures of the pure components, the eutectic and the monotectic were recorded [16] by placing a drop of molten compound on a hot glass slide. To avoid the inclusion of the impurities from the atmosphere, a cover slip was glided over the melt and it was allowed to cool to get a supercooled liquid. The melt was nucleated with a seed crystal of the same composition at one end and also the care was taken to have unidirectional freezing. The unidirectional solidify microstructure was then placed on the platform of an optical microscope (Leitz Labourlux D). The different regions of microstructure were viewed and photographs of interesting region were taken choosing suitable magnification of camera attached with the microscope.

3. Results and discussion

3.1. Phase diagram

The phase diagram of the R–DIB system shows the formation of a monotectic and a eutectic where the mole fraction of R is 0.05 and 0.97, respectively (Fig. 1). The eutectic and the monotectic

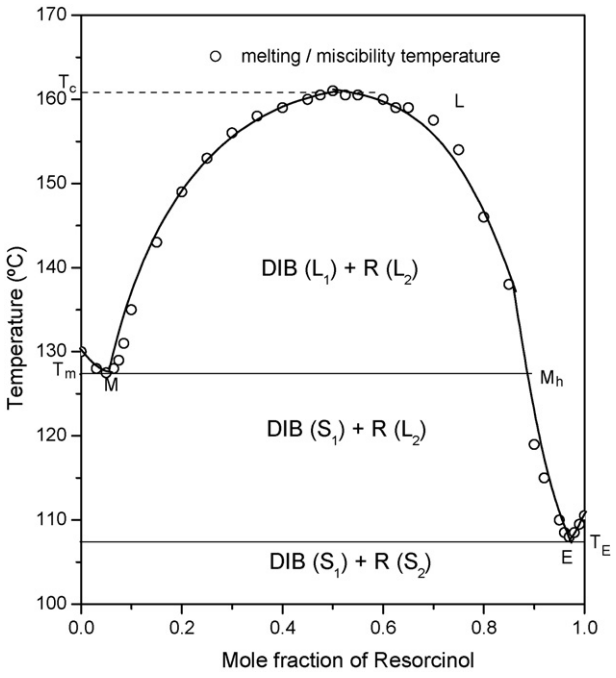

Fig. 1. Phase diagram of resorcinol–1,4-diiodobenzene system. Melting/miscibility temperature.

melting temperatures correspond to 108.0 and 127.5 °C, respectively. The upper consolute/critical temperature (T_c) is 161.0 °C which is 33.5 °C above the monotectic horizontal (M_h). Above the critical temperature (T_c), the two components are miscible in all proportions. However, below T_c temperature and between a certain compositions range the two immiscible liquids (L_1 and L_2) are produced. When a liquid of monotectic composition (M) is cooled through the monotectic horizontal (T_M), the monotectic reaction occurs where a liquid L_1, which is rich in DIB, decomposes into a solid phase rich in DIB and another liquid phase L_2 (rich in R). At the monotectic temperature the reaction which occurs isothermally is

$$L_1 \leftrightharpoons S_1 + L_2. \quad (1)$$

When the liquid of eutectic composition is allowed to cool below the eutectic horizontal (T_E), eutectic reaction takes place in which eutectic liquid decomposes into two solids. The eutectic reaction, occurring isothermally, can be shown as

$$L_2 \leftrightharpoons S_1 + S_2 \quad (2)$$

The monotectic reaction is similar to the eutectic reaction expect that one of the product phases of the monotectic reaction is a second liquid phase. The melting points of DIB and R are 130.0 and 110.5 °C, respectively.

3.2. Study of solid solution formation

The X-ray diffraction patterns of pure R, DIB and their monotectic, eutectic and a particular composition (0.15 mole fraction of R), which is beyond the monotectic, were recorded. The variable parameters of XRD unit were kept constant for each sample. The XRD patterns of different samples are shown in Fig. 2. It is evident from the figure that the XRD pattern of DIB and monotectic composition (Fig. 2(d) and (e), respectively) is identical barring a nominal change in intensity of few of the peaks. On the other side, the compositions up to eutectic point show the similar XRD pattern to that of R (Fig. 2(a) and (b)). While in the powder XRD pattern of a composition (0.15 mole fraction of R) beyond monotectic, the peaks indexed were identified for both DIB and R (Fig. 2(c)), which

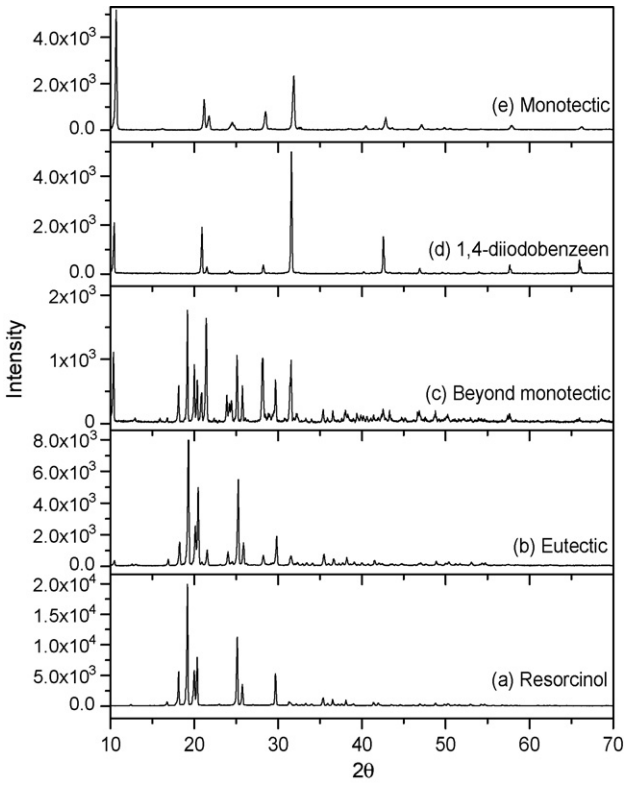

Fig. 2. Powder XRD of resorcinol, 1,4-diodobenzene and their monotectic, eutectic and beyond monotectic.

infers that this composition is of mechanical mixture nature similar to binary composite. From these findings of identical XRD of monotectic to that of DIB, and eutectic to that of R conclude that the monotectic and DIB are isostructure as well as eutectic and R is isostructure. Therefore, the compositions starting from zero to 0.05 mole fraction of R in DIB and from zero to 0.03 mole fraction of DIB in R form the solid solution [18,20]. Both solids, DIB and R, are soluble in each other in a short proportion. The maximum solubility of R in DIB is up to the monotectic composition only, however the solubility of DIB in R is only possible up to the eutectic composition (Fig. 1). The particular compositions where the mole fraction of R is 0.05 and DIB is 0.03 are the monotectic and eutectic points, respectively.

3.3. Growth kinetics

In order to study the crystallization behaviour of the pure components, the eutectics and the monotectics the crystallization rate (v) are determined at different undercoolings (ΔT) by measuring the rate of movement of solid-liquid interface in a capillary. The plots between $\log \Delta T$ and $\log v$ are given in Fig. 3. The linear dependence of these plots is in accordance with the Hillig and Turnbull [21] equation:

$$v = u(\Delta T)^n. \quad (3)$$

where u and n are constants and depend on the solidification behaviour of the materials involved. The values of u and n are given in Table 1. These findings may be explained by the mechanism given by Winegard et al. [22] where the crystallisation of eutectic/monotectic begins with the formation of the nucleus of one of the phases. This phase grows until the surrounding liquid becomes rich in the other component and a stage is reached when the second component start nucleating. Now there are two possibilities, either the two initial crystals grow side-by-side or there

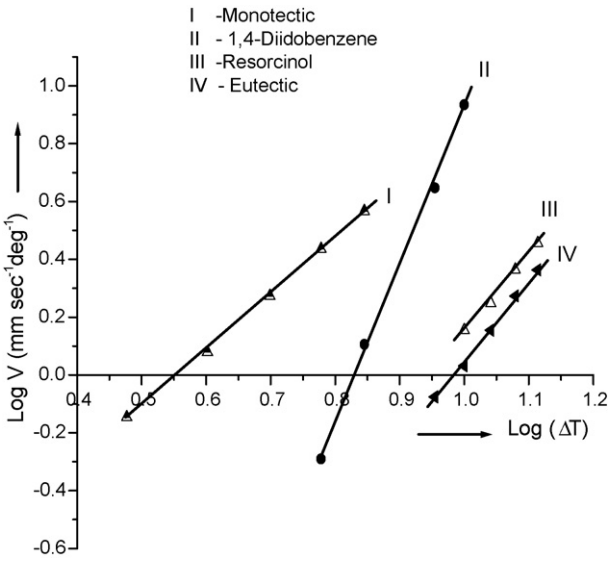

Fig. 3. Linear velocity of crystallisation at various degrees of undercooling for resorcinol, 1,4-diiodobenzene and their eutectic and monotectic.

may be alternate nucleation of the two phases. The values of n for the monotectic being close to 2 suggest that there is square relationship between growth velocity and undercoolings. The deviation of n values from 2 observed in some cases is due to difference in temperature of bath and temperature of growing interface. From the values of u (Table 1) it can be concluded that growth velocity of eutectic lies between those of the parent components, however for monotectic it is higher than the parent components. These findings suggest that the two phases of monotectic and eutectic solidify by the side-by-side growth mechanism.

3.4. Thermochemistry

The knowledge of enthalpy of fusion values of the pure components, the eutectic and the monotectic are important in understanding the mechanism of solidification, structure of eutectic melt and the nature of interaction between two components forming the eutectic and the monotectic. The values of enthalpy of fusion of the pure components, the eutectic and the monotectic, determined by the DSC method, are reported in Table 2. For comparison, the value of enthalpy of fusion of eutectic calculated by the mixture law [16] is also included in the same table. The enthalpy of mixing which is the difference of experimental and the calculated values of the enthalpy of fusion are found to be 0.73 kJ mol^{-1}. As such, three types of structures are suggested [23]; quasi-eutectic for $\Delta_{mix}H > 0$, clustering of molecules for $\Delta_{mix}H < 0$ and molecular solution for $\Delta_{mix}H = 0$. In present system the positive value of $\Delta_{mix}H$ for the eutectic suggests the formation of quasi-eutectic structure in the binary melt of the eutectic [24]. The entropy of fusion ($\Delta_{fus}S$) values, for different materials has been calculated by dividing the enthalpy of fusion by their corresponding absolute melting temperatures (Table 2). The positive values suggest that the entropy factor favours the melting process.

Table 1
Values of n and u for pure components, monotectic and eutectic.

Material	n	u (mm s^{-1} deg^{-1})
R	2.7	2.93×10^{-3}
DIB	5.4	3.25×10^{-5}
Monotectic	1.9	8.2×10^{-2}
Eutectic	2.8	1.72×10^{-3}

Table 2
Heat of fusion, entropy of fusion and roughness parameter.

Materials	Heat of fusion (kJ mol^{-1})	Heat of mixing (kJ mol^{-1})	Entropy of fusion (J mol^{-1} K^{-1})	Roughness parameter (α) (kJ mol^{-1} K^{-1})
R	22.20		57.89	6.96
DIB	24.13		59.88	7.20
Monotectic				
Exp.	23.79		59.40	7.14
Eutectic				
Exp.	22.99	0.73	60.03	7.25
Cal.	22.26			

The deviation from the ideal behaviour can best be expressed in terms of excess thermodynamic functions, namely, excess free energy (g^E), excess enthalpy (h^E), and excess entropy (s^E) which give a more quantitative idea about the nature of molecular interactions. The excess thermodynamic functions could be calculated [16,25] by using the following equations and the values are given in Table 3:

$$g^E = RT[x_1 \ln \gamma_1^1 + x_2 \ln \gamma_2^1] \quad (4)$$

$$h^E = -RT^2 \left[x_1 \frac{\partial \ln \gamma_1^1}{\partial T} + x_2 \frac{\partial \ln \gamma_2^1}{\partial T} \right] \quad (5)$$

$$s^E = -R \left[x_1 \ln \gamma_1^1 + x_2 \ln \gamma_2^1 + x_1 T \frac{\partial \ln \gamma_1^1}{\partial T} + x_2 T \frac{\partial \ln \gamma_2^1}{\partial T} \right] \quad (6)$$

where $\ln \gamma_i^1$, x_i and $\partial \ln \gamma_i^1/\partial T$ are activity coefficient in liquid state, the mole fraction and variation of log of activity coefficient in liquid state as function of temperature of the component i.

It is evident from Eqs. (4)–(6) that activity coefficient and its variation with temperature are required to calculate the excess functions. Activity coefficient (γ_i^1) could be evaluated [16,26] by using the equation

$$-\ln(x_i \gamma_i^1) = \frac{\Delta_{fus} H_i}{R} \left(\frac{1}{T_{fus}} - \frac{1}{T_i} \right) \quad (7)$$

where x_i, $\Delta_{fus}H_i$, T_i and T_{fus} are mole fraction, enthalpy of fusion, melting temperature of component i and melting temperature of eutectic, respectively. The variation of activity coefficient with temperature could be calculated by differentiating equation (7) with respect to temperature

$$\frac{\partial \ln \gamma_i^1}{\partial T} = \frac{\Delta_{fus} H_i}{RT^2} - \frac{\partial x_i}{x_i \partial T} \quad (8)$$

$\partial x_i/\partial T$ in this expression can be evaluated by considering two points around the eutectic. The positive values of excess free energy indicate that the interaction between the like molecules are stronger than the interaction between the unlike molecule [25].

The solid–liquid interfacial tension affects the enthalpy of fusion value and plays an important role in determining the kinetics of phase transformation. When liquid is cooled below its melting temperature, the melt does not solidify spontaneously because under equilibrium condition, it contains number of clusters of molecules of different sizes. As long as the clusters are well below the critical size [27], they cannot grow to form crystals and, therefore, no solid would result. Also during growth, the radius of critical nucleus gets influenced by undercooling as well as the interfacial energy. The interfacial energy (σ) is given by

$$\sigma = \frac{C \Delta_{fus} H}{(N_A)^{1/3} (V_m)^{2/3}} \quad (9)$$

where N_A is the Avogadro number, V_m is the molar volume, and parameter C lies between 0.30 and 0.35.

The calculated values of interfacial energy using equation are given in Table 3. The literature [28,29] during the past two decades is replete with various attempts to understand and to explain the process of solidification of monotectic alloys. The role of wetting behaviour in a phase separation process is of immense important. In view of this, the applicability of Cahn's wetting condition has been tested in the present case. The values of interfacial energy (Table 4) in present case show applicability of non-wetting condition by satisfying the relation

$$\sigma_{SL_2} > \sigma_{SL_1} + \sigma_{L_1L_2} \quad (10)$$

where σ is the interfacial energy between the faces denoted by the subscripts. The interfacial energy between two liquids, $\sigma_{L_1L_2}$, has been calculated using the equation

$$\sigma_{L_1L_2} = \sigma_{SL_1} + \sigma_{SL_2} - \sqrt{\sigma_{SL_1} \sigma_{SL_2}} \quad (11)$$

To study the critical nucleus (r^*) and the influence of undercooling on it, the following equation was used

$$r* = \frac{2\sigma T_{fus}}{\Delta_{fus} H \cdot \Delta T} \quad (12)$$

where T_{fus}, $\Delta_{fus}H$ and ΔT are melting temperature of eutectic, heat of fusion and degree of undercooling, respectively. The computed values of the size of critical nucleus at different undercoolings using Eqs. (9) and (12) are given in Table 5. The size of critical nucleus

Table 3
Excess thermodynamic functions for the eutectic.

Material	g^E (kJ mol^{-1})	h^E (kJ mol^{-1})	s^E (J mol^{-1} K^{-1})
DIB–R eutectic	0.2470	17.9349	46.43

Table 4
Interfacial energy of resorcinol, 1,4-diiodobenzene, eutectic and monotectic.

Parameter	Interfacial energy (ergs cm^{-1})
σ_{SL_2} (R)	47.17
σ_{SL_1} (DIB)	38.27
$\sigma_{L_1L_2}$ (DIB–R)	0.47
σ_E (DIB–R)	46.89

Table 5
Critical radius of resorcinol, 1,4-diiodobenzene, eutectic and monotectic.

Undercooling	Critical radius $\times 10^{-8}$ (cm)			
ΔT (°C)	R	DIB	Monotectic	Eutectic
3.0			0.052	
4.0			0.039	
5.0			0.031	
6.0		2.130	0.026	
7.0		1.831	0.022	
9.0		1.424		1.727
10.0	1.629	1.281		1.554
11.0	1.481			1.413
12.0	1.358			1.295
13.0	1.253			1.195

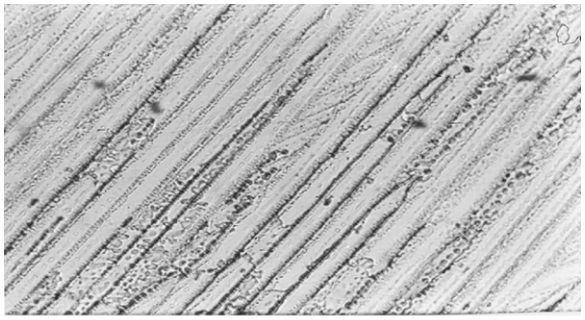

(a) Microstructure of monotectic X 220

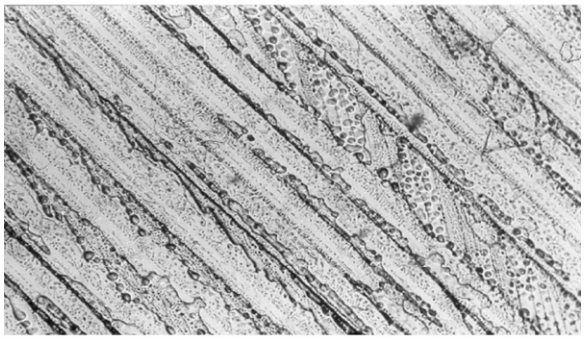

(b) Microstructure of eutectic X 220

Fig. 4. Directionally solidify optical microphotograph of resorcinol–1,4-diiodobenzene monotectic (a) and (b) eutectic.

decreased with increase in undercooling. Thus high undercooling favours the formation of critical nucleus of smaller size. This may be ascribed to the increase amplitude of molecular vibration at higher temperature.

3.5. Microstructure

In polyphase materials the microstructure gives information about shape and size of the crystallites, which play a significant role in deciding the mechanical, electrical, magnetic and optical properties of materials. According to Hunt and Jackson [30] the type of growth from melts depends upon the interface roughness (α) defined by

$$\alpha = \xi\Delta_{\text{fus}} \cdot \frac{H}{RT} \tag{13}$$

where ξ is a crystallographic factor which is generally equal to or less than one. The values of α are reported in Table 2. If $\alpha > 2$ the interface is quite smooth and the crystal develops with a faceted morphology. On the other hand, if $\alpha < 2$, the interface is rough and many sites are continuously available and the crystal develops with a non-faceted morphology. In the present system, the values of α are greater than 2 in all the cases which suggests that the phases grow with facets morphology.

3.5.1. Microstructure of monotectic and eutectic

The microstructure of monotectic and eutectic is given in Fig. 4. The study of interfacial energy reveals the applicability of non-wetting condition, i.e., both phases are not wetting to each other. The effect of non-wetting could be seen clearly from the microstructure of monotectic and eutectic. The microstructure of monotectic (Fig. 4(a)) shows that one phase (DIB) has solidify with lamellar morphology; however resorcinol has solidify with droplets morphology near the lamella. On the other hand, microstructure of eutectic (Fig. 4(b)) also shows that DIB has solidify with thinner lamellar morphology along with bigger droplets of another phase (R). In the microstructure of monotectic and eutectic, the thickness of lamella and droplets size infers the proportion of DIB and R. The closer view of microstructures shows that to minimize the surface energy, the tendency of droplets is to be spherical shape. In some region the spherical drops and being observed while some region of microstructure shows elongated spherical structures. This may be due to the reason that time of formation of sphere is more than the freezing time.

4. Conclusions

The phase diagram between resorcinol and 1,4-diiodobenzene shows the formation of a monotectic and a eutectic with 0.05 and 0.97 mole fractions of resorcinol, respectively. The diagram shows that upper consolute temperature is 33.5 °C above the monotectic horizontal. The DIB and R are miscible in each other up to a convinced limit and form the solid solution. The growth kinetics suggests that growth data obey the Hillig–Turnbull equation for each material, and the size of critical nucleus depends on the undercoolings. The enthalpy of mixing and excess free energy was found to be positive. The interfacial energies are correlated by the relation $\sigma_{SL_2} > \sigma_{SL_1} + \sigma_{L_1L_2}$, which confirms the Cahn's non-wetting condition is applicable to the present system. The microstructural investigations show lamellar growth morphology for one phase and droplets morphology for other phase, and both could appear together which further chains the finding of non-wetting condition.

Acknowledgements

The authors would like to thank Board of Research in Nuclear Science, Department of Atomic Energy, Mumbai, India for financial support.

References

[1] D.M. Herlach, R.F. Cochrane, I. Egry, H.J. Fecht, A.L. Greer, Int. Mater. Rev. 38 (1993) 273–347.
[2] B. Predel, J. Phase Equilibr. 18 (4) (1997) 327–337.
[3] R. Trivedi, W. Kurz, Int. Mater. Rev. 39 (2) (1994) 49–74.
[4] B. Majumdar, K. Chattopadhyay, Metall. Trans. A 27 (A) (1996) 2053–2057.
[5] M.E. Glicksman, N.B. Singh, M. Chopra, Manuf. Space 11 (1983) 207–218.
[6] H. Yasuda, I. Ohnaka, Y. Matsunaga, Y. Shiohara, J. Cryst. Growth 158 (1996) 128–135.
[7] K. Pigon, A. Krajewska, Thermochim. Acta 58 (1982) 299–309.
[8] S. Akbulut, Y. Ocak, U. Boyiik, K. Keslioglu, N. Marash, J. Phys.: Condens. Matter 18 (2006) 8403–8412.
[9] J.P. Farges, Organic Conductors, Marcel Dekker, Inc., New York, 1994.
[10] P. Gunter, Nonlinear Optical Effects and Materials, Springer-Verlag, Berlin, 2000, p. 540.
[11] N.B. Singh, T. Henningsen, R.H. Hopkins, R. Mazelsky, R.D. Hamacher, E.P. Supertzi, F.K. Hopkins, D.E. Zelmon, O.P. Singh, J. Cryst. Growth 128 (1993) 976–980.
[12] B. Derby, J.J. Favier, Acta Metall. 7 (1983) 1123–1130.
[13] A. Ecker, D.O. Frazier, J.I.D. Alexander, Metall. Trans. 20A (1989) 2517–2527.
[14] J.A. Dean, Lange's Handbook of Chemistry, McGraw-Hill, New York, 1985.
[15] Lulinski Piotr, Barbara Krassowska-Swiebocka and Lech Skulski Molecules 9 (2004) 595–601.
[16] R.N. Rai, J. Mater. Res. 99 (5) (2004) 1348–1355.
[17] U.S. Rai, R.N. Rai, Chem. Mater. 11 (11) (1999) 3031–3036.
[18] N. Imanaka, M. Hiraiwa, S. Tamura, G. Adachi, H. Dabkowska, A. Dabkowski, J. Cryst. Growth 208 (2000) 466–470.
[19] U.S. Rai, R.N. Rai, J. Thermal Anal. Calorim. 53 (1998) 883–893.
[20] J.M. Calderon-Moreno, Y. Masahiro, Solid State Ion. 154–155 (2002) 125–133.
[21] W.B. Hillig, D. Turnbull, J. Chem. Phys. 24 (1956) 914.
[22] W.C. Winegard, S. Majka, B.M. Thall, B. Chalmers, Can. J. Chem. 29 (1951) 320–327.
[23] R.N. Rai, U.S. Rai, Thermochim. Acta 363 (2000) 23–28.
[24] U.S. Rai, R.N. Rai, J. Cryst. Growth 191 (1998) 234–242.
[25] N. Singh, B. Singh Narsingh, U.S. Rai, O.P. Singh, Thermochim. Acta 95 (1985) 291–293.
[26] R.N. Rai, U.S. Rai, K.B.R. Varma, Thermochim. Acta 387 (2002) 101–107.
[27] J.W. Christian, The Theory of Phase Transformation in Metals and Alloys, Pergamon Press, Oxford, 1965, p. 992.
[28] W.F. Kaukler, D.O. Frazier, J. Cryst. Growth 71 (1985) 340–345.
[29] N.B. Singh, U.S. Rai, O.P. Singh, J. Cryst. Growth 71 (1985) 353–360.
[30] J.D. Hunt, K.A. Jackson, Trans. Metall. Soc. AIME 236 (1966) 843–852.